How to cite: *Angew. Chem. Int. Ed.* **2021**, *60*, 25372–25380
International Edition: doi.org/10.1002/anie.202109642
German Edition: doi.org/10.1002/ange.202109642

Hydrogenation Catalysts | Hot Paper

Reduction of Nitrogen Oxides by Hydrogen with Rhodium(I)–Platinum(II) Olefin Complexes as Catalysts

Pascal Jurt, Anne Sofie Abels, Juan José Gamboa-Carballo, Israel Fernández, Grégoire Le Corre, Marcel Aebli, Matthew G. Baker, Frederik Eiler, Fabian Müller, Michael Wörle, René Verel, Sébastien Gauthier, Monica Trincado, Thomas L. Gianetti,* and Hansjörg Grützmacher**

Abstract: *The nitrogen oxides NO_2, NO, and N_2O are among the most potent air pollutants of the 21st century. A bimetallic Rh^I–Pt^{II} complex containing an especially designed multidentate phosphine olefin ligand is capable of catalytically detoxifying these nitrogen oxides in the presence of hydrogen to form water and dinitrogen as benign products. The catalytic reactions were performed at room temperature and low pressures (3–4 bar for combined nitrogen oxides and hydrogen gases). A turnover number (TON) of 587 for the reduction of nitrous oxide (N_2O) to water and N_2 was recorded, making these Rh^I–Pt^{II} complexes the best homogeneous catalysts for this reaction to date. Lower TONs were achieved in the conversion of nitric oxide (NO, TON = 38) or nitrogen dioxide (NO_2, TON of 8). These unprecedented homogeneously catalyzed hydrogenation reactions of NO_x were investigated by a combination of multinuclear NMR techniques and DFT calculations, which provide insight into a possible reaction mechanism. The hydrogenation of NO_2 proceeds stepwise, to first give NO and H_2O, followed by the generation of N_2O and H_2O, which is then further converted to N_2 and H_2O. The nitrogen–nitrogen bond-forming step takes place in the conversion from NO to N_2O and involves reductive dimerization of NO at a rhodium center to give a hyponitrite ($N_2O_2^{2-}$) complex, which was detected as an intermediate.*

Introduction

Nitrogen oxides such as N_2O (nitrous oxide), NO (nitric oxide), and NO_2 (nitrogen dioxide) are potent greenhouse gases and a hazard to human health. Because NO readily oxidizes to NO_2 in air, the effect of NO and NO_2 on climate and human health is frequently discussed jointly by referring to NO_x as toxic pollutants. N_2O and NO_x have high global warming potentials of 298[1] and 126[2] CO_2 equivalents, respectively. Additionally, N_2O has been identified as the dominant ozone-depleting agent of the 21st century.[3] NO_x facilitates the formation of certain respiratory diseases and cancers, especially in densely populated areas.[4] Significant amounts of nitrogen oxides in the atmosphere are of natural origin (64% for N_2O and 16% for NO_x). Since the start of the industrial revolution, emissions from non-natural sources have increasingly contributed to the overall atmospheric concentration. The combustion of fossil fuels is the main source of NO_x in our atmosphere (64%). N_2O is a waste product from chemical processes (6%),[5] predominantly from adipic[6] and nitric acid syntheses.[7] Furthermore, denitrification from nitrogen-containing fertilizers, derived from the Haber-Bosch process, adds 30% N_2O and 20% NO_x to the atmospheric concentration.[8]

Mitigation of these gases is crucial for both, slowing down global warming and improving the health of all living populations. N_2O, NO, and NO_2 are thermodynamically unstable concerning their decomposition in N_2 and O_2

[*] Dr. P. Jurt, A. S. Abels, J. J. Gamboa-Carballo, G. Le Corre, M. Aebli, Dr. M. G. Baker, F. Eiler, Dr. F. Müller, Dr. M. Wörle, Dr. R. Verel, Dr. M. Trincado, Prof. Dr. T. L. Gianetti, Prof. Dr. H. Grützmacher
Department of Chemistry and Applied Biosciences, ETH
Vladimir-Prelog-Weg 1, CH-8093 Zurich (Switzerland)
E-mail: trincado@inorg.chem.ethz.ch
hgruetzmacher@ethz.ch

J. J. Gamboa-Carballo
Higher Institute of Technologies and Applied Sciences (InSTEC)
University of Havana
Ave. S. Allende 1110, 10600 Havana (Cuba)

I. Fernández
Departamento de Química Orgánica I and Centro de Innovación en Química Avanzada (ORFEO-CINQA), Facultad de Ciencias Químicas, Universidad Complutense de Madrid
28040 Madrid (Spain)

Dr. S. Gauthier
Univ. Rennes, CNRS, ISCR (Institut des Sciences Chimiques de Rennes)—UMR 6226
F-35000 Rennes (France)

Prof. Dr. T. L. Gianetti
Department of Chemistry and Biochemistry
University of Arizona, Tucson
1306 E. University Blvd., Tucson, AZ 85719 (USA)
E-mail: tgianetti@arizona.edu

Supporting information and the ORCID identification number(s) for the author(s) of this article can be found under: https://doi.org/10.1002/anie.202109642.

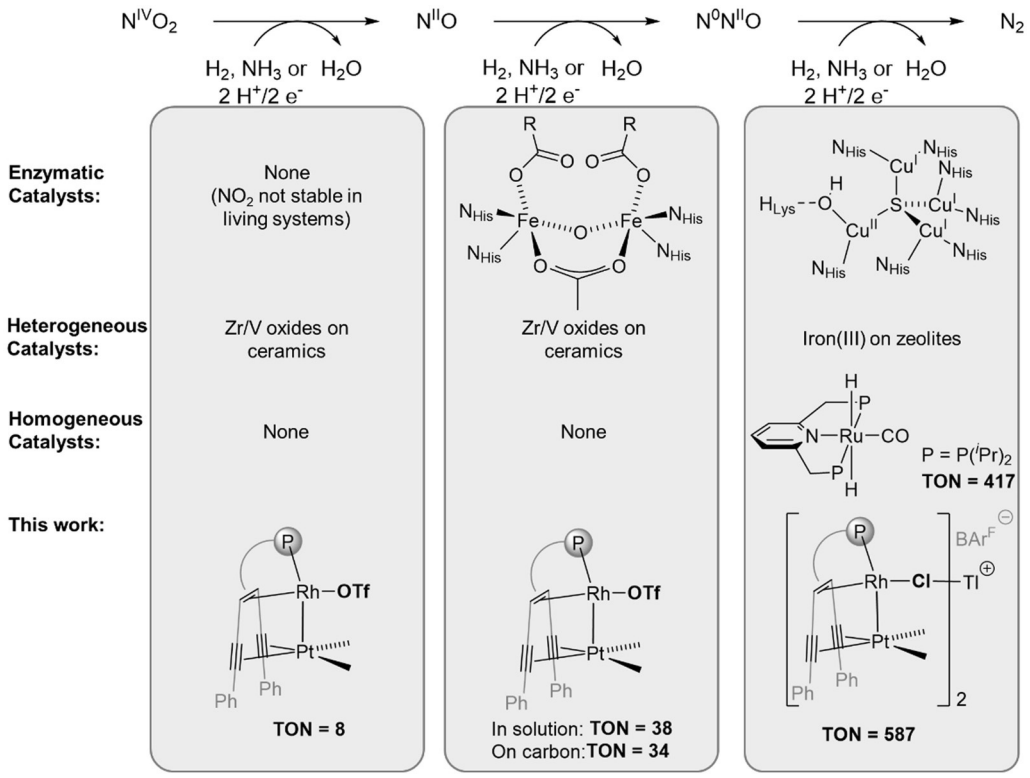

Figure 1. State-of-the-art catalysts for the reduction of the nitrogen oxides NO_2, NO and N_2O with H_2, NH_3 or H_2O as reagents. Enzymatic, heterogeneous, and homogeneous examples are presented alongside the homogeneous and heterogenized catalysts presented in this work.

($\Delta_f H^0(298\,K) = 82$, 90 and 33 kJ mol^{-1}),[9] but high activation barriers for these processes make them kinetically inert. Various heterogeneous catalysts[10] have been developed to catalyze their conversion to nitrogen and oxygen, but high temperatures and pressures are required. Such catalytic systems were used for decades in after-treatment systems of exhaust lines of combustion engines.[11] However they are not suited to fit modern-day regulations,[12] which led to the development of new types of converters in which NO_x is reduced predominantly by ammonia (Figure 1).[13]

Currently, hydrogen is still produced mainly by methane steam reforming but due to large research efforts into the development of power-to-gas technologies, inexpensive hydrogen from renewable sources will become available soon.[14] Hence, it might become a promising atom-economic reducing agent for the mitigation of N_2O and NO_x. Several heterogeneous catalysts successfully hydrogenate N_2O,[15] but there are only two homogeneous catalysts containing rhodium[16] or ruthenium which promote this reaction (TONs up to 417).[17] To the best of our knowledge, no homogeneous catalytic system has been reported for the catalytic reduction of NO or NO_2 with hydrogen. Only stoichiometric reactions with iron,[18] nickel,[19] copper,[20] or ruthenium complexes were reported recently.[21] Nature has developed a set of enzymes that can catalyze the reduction of N_2O and NO.[22] NO can be reduced by iron-containing nitric oxide reductases and the bimetallic active core of one of these is presented in Figure 1. In such enzymes, NO can be reduced to N_2O. The reduction of N_2O by nitrous oxide reductase, which contains a Cu_4S cluster as the active site, also relies on cooperativity between two copper centers: N_2O is first chelated between two copper centers followed by N_2 extrusion.[22a]

Inspired by the high stability of catalytic converters that contain rhodium, palladium or platinum,[11] and the bimetallic cooperativity observed in nature,[22] we synthesized a series of Rh^I–Pt^{II} complexes using a special $^{(PhC\equiv C)_2}$tropPPh$_2$ (trop = 5*H*-dibenzo[*a*,*d*]cyclohepten-5-yl) ligand. These complexes were analyzed by X-ray diffraction methods and multinuclear NMR spectroscopy in order to determine their structures. Subsequently, these bimetallic complexes were tested in the reduction of N_2O with hydrogen. In addition, selected complexes were also examined in the reduction of NO and NO_2. Finally, a series of stoichiometric and catalytic hydrogenation reactions were performed which, combined with results from DFT calculations, give insight into a possible reaction mechanism.

Results and Discussion

Synthesis and characterization of heterobinuclear Rh–Pt complexes

The multidentate ligand **1** (Figure 2a) was synthesized by adapting a recently published protocol (Supporting Information, Figure S1).[23] The ligand is designed in such a way that two transition metals can bind in close proximity within the concave pocket formed by the diphenylphosphino group, Ph_2P, the alkene unit of the central seven-membered ring, and the two alkynyl units. The first metal is introduced by reacting

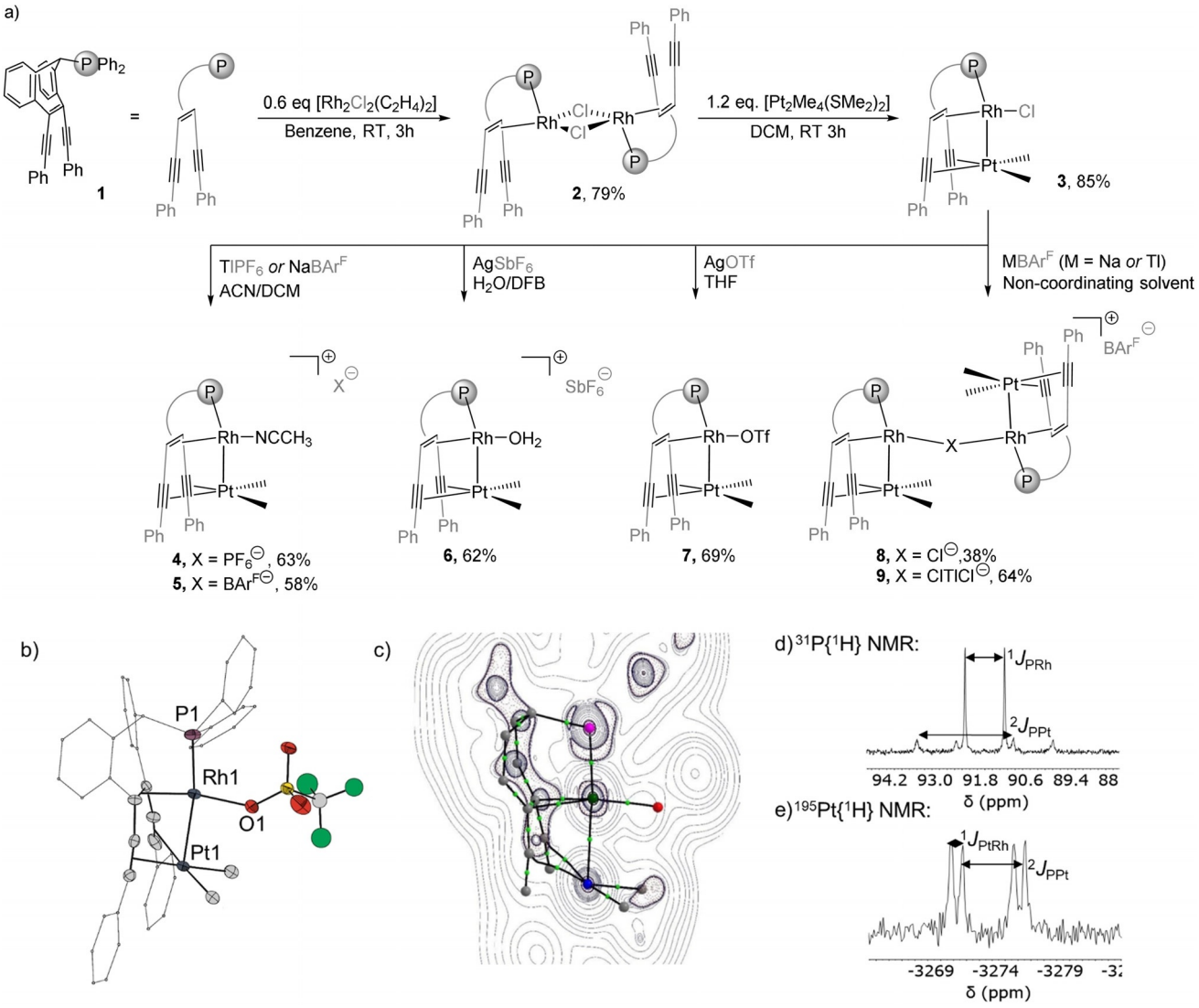

Figure 2. a) Synthesis of complexes **2–9** starting from ligand **1**. b) Plot of the molecular structure of **7** determined by X-ray diffraction methods (hydrogen atoms and two molecules of tetrahydrofuran are omitted for clarity). c) Contour plot for the Laplacian of the electron density ($\nabla^2\rho$) of **7** in the P-Rh-Pt plane. Only relevant atoms are shown. Solid lines indicate electron concentration, dotted lines electron depletion. Bond critical points are indicated as green dots. d) $^{31}P\{^1H\}$ NMR and e) $^{195}Pt\{^1H\}$ NMR spectra of complex **7**.

1 with $[Rh_2(\mu_2\text{-}Cl)_2(C_2H_4)_4]$ in benzene which gives the chloro-bridged dimeric rhodium complex **2** in good yield (Figure 2a). Subsequent reaction with $[Pt_2Me_4(\mu_2\text{-}SMe_2)_2]$ in dichloromethane cleanly gives the heterobimetallic complex **3** in 85% isolated yield. Various salts such as M(PF_6), M(BAr^F) {M = Na, Tl; $BAr^F = B[(3,5\text{-}CF_3)_2C_6H_3]_4^-$} or Ag(X) ($X = SbF_6^-$, $OTf^- = CF_3SO_3^-$) were tested as chloride scavenger agents and reacted with **3**. In the presence of coordinating solvents such as acetonitrile or water, complexes **4–6** were obtained (Figure 2a). The reaction between **3** and AgOTf leads to **7** which contains OTf^- as weakly coordinating anion bound to the Rh center. Remarkably, the reaction in a non-coordinating solvent such as benzene or toluene leads to the dimeric aggregates **8** and **9** in which two [RhPt($Me)_2$(**1**)] units are bridged via a Cl^- ion or a $TlCl_2^-$ ion. All complexes were obtained as deep red crystals in moderate to good yields and their molecular structures were determined by X-ray diffraction analysis of single crystals (Figures S3–S10).

Multinuclear NMR spectroscopy including ^{103}Rh and ^{195}Pt NMR spectroscopy, was used to characterize these complexes in solution (Figures S18–S64). As an example, a structure plot of the triflate complex **7** is shown in Figure 2b. Remarkably, complex **9** shows an interaction between the central Tl^+ ion and two phenyl groups of the PPh_2 units (Tl-*ct* = 3.2147(18) Å; *ct* = centroid of the phenyl groups; Figure S10). This interaction is retained in solution as indicated by an resonance signal at δ $^{205}Tl = -699$ ppm in the ^{205}Tl NMR spectrum in [D_8]THF (Figure S64), which is comparable with previously reported data for Tl^I diarene complexes (e.g. $[Tl(hexamethylbenzene)_2]^+$: δ $^{205}Tl = -563$ ppm, vs. TlCl: δ $^{205}Tl = 383$ ppm).[24] This low-frequency chemical shift is likely caused by ring current effects within the arene rings.[25]

The structural data collected for complexes **3**–**9** (Figures S3–S10) reveal distances between the two metal centers (2.67–2.77 Å; Figure S65) which are in line with previously reported Rh^{I}–Pt^{II} bond lengths (2.63–2.98 Å).[26] The short Rh–Pt distances, the $^{2}J_{PPt}$ coupling constants of $^{2}J_{PPt} = 506$–538 Hz, and the direct $^{1}J_{PtRh}$ coupling of $^{1}J_{PtRh} = 82$–104 Hz observed by ^{195}Pt NMR spectroscopy (Figures S26–S63) are strong indications for a Rh−Pt bond. Although the NMR data are relatively invariant for **3**–**9**, the shorter Rh−Pt bonds in the cationic monomeric complexes **4**–**6** (Rh−Pt ≤ 2.70 Å) correlate with a slightly larger $^{1}J_{PtRh}$ coupling constant (> 97 Hz; Supporting Information, Table S1). Theoretical methods were employed to further characterize the Rh−Pt bond. An analysis of the electronic structure of **7** using the quantum theory of atoms in molecules (QTAIM) (Figure 2c) supports the assumption that the Rh−Pt interaction is a direct metal−metal bond as indicated by the bond critical point on the path of maximum electron density between Rh and Pt (Figure 2b). In addition, the positive value of the corresponding Laplacian of the electron density computed at such bond critical point ($\nabla^2\rho = +0.13$) suggests that the Rh−Pt bond is best described as a closed-shell (donor–acceptor) interaction. A molecular orbital—linear combination of atomic orbitals (MO-LCAO) analysis (Figure S66) and an energy decomposition analysis combined with the natural orbitals for chemical valency (EDA-NOCV, Figure S67) indicate that the Rh−Pt bond is indeed best described as a donor–acceptor interaction in which the d^{8}-Pt^{II} center acts as a donor through its doubly occupied dz^2-orbital (Figure S68, Table S2).

Catalytic reduction of N_2O

Complexes **3**–**9** were tested in the catalytic reduction of N_2O in tetrahydrofuran with hydrogen at an overall pressure of 2 bar (room temperature, one bar partial pressure of N_2O or hydrogen, respectively, Table 1). The turnover number (TON) was determined by ^{1}H NMR spectroscopy by quantification of the proton signals of water as one of the products (Supporting Information). Nitrogen as the sole further product was detected in the final reaction mixture by gas chromatography with a thermal conductivity detector (GC-TCD). All catalysts are stable under the reaction conditions and no decomposition was observed by ^{31}P NMR spectroscopy after the catalytic reaction ceased (Figure S70). Catalyst **7** remains active for more than two days without significant loss in catalytic activity (Figure S71). Under these very mild reaction conditions, the complexes showed TONs between 10 and 140 in tetrahydrofuran (Table 1, Entry 1–7). Changing the solvent from tetrahydrofuran to dichloromethane resulted in a lower TON of 12 (using complex **7** as catalyst) while in benzene, hydrogenation of the solvent to cyclohexane instead of N_2O was observed. Comparing the catalytic activity of complexes **3**–**9** shows that the aquo complex **6** and the ClTlCl-bridged complex **9** are the best performing catalysts (Table 1, entries 4 and 7). Even at temperatures as low as 0 °C, TON of up to 151 were obtained with catalysts **9** (Table S3). These results indicate that a weakly bound ligand at the rhodium center as in complexes

Table 1: Catalytic reduction of N_2O by complexes **3**–**10**.[a]

$N_2O + H_2 \xrightarrow[\textbf{[RhPt]}]{\text{THF, RT, 22-48 h}} H_2O + N_2$

Entry	[RhPt]	t [h]	p[b] [bar]	TON[c]
1	**3**	22	1	11
2	**4**	22	1	10
3	**5**	22	1	11
4	**6**	22	1	135
5	**7**	22	1	62
6	**8**	22	1	34[d]
7	**9**	22	1	140[d]
8	**9** + 50 equiv. PPh_3	22	1	9
9	**3** + $AgSbF_6$[e]	22	1	36
10	**10**[f]	22	1	10
11	**6**	48	2	475
12	**9**	22	2	250[d]
13	**9**	48	2	587[d]

[a] Conditions: [cat.] (3.5 mM), tetrahydrofuran (2 mL), total volume (120 mL). [b] Partial pressure of both gases. [c] Water formed during the reaction determined by ^{1}H NMR spectroscopy with mesitylene as an internal standard. [d] With respect to one RhPt core. [e] Generated in situ (see the Supporting Information for details). [f] Monomeric rhodium complex [$^{(TMSC\equiv C)_2}$TropPPh$_2$RhPPh$_3$]OTf (Figure S69).

6 (H_2O), **7** (OTf^-) and **9** ($TlCl_2^-$) ensures efficient catalysis suggesting that an easily accessible coordination site at the Rh center is required. This conclusion is further supported by the enhanced activity when **3** is reacted with a chloride abstracting agent such as $AgSbF_6$ leading to an increase of TON values of 11 to 36 (Table 1, entry 9). On the contrary, the addition of a complexing agent such as PPh_3 inhibits the hydrogenation of N_2O (Table 1, entry 8) which also indicates that the catalysis proceeds in homogeneous solution.[27] Finally, the mononuclear rhodium complex in which the two-electron donating $PtMe_2$ fragment is replaced by PPh_3, [Rh($^{(TMSC\equiv C)_2}$tropPPh$_2$)(PPh$_3$)](OTf) **10**,[23] has low activity (TON = 10, Table 1, entry 10). This result indicates that the $PtMe_2$ fragment is important as structural and electronic modulator as well as cooperative metal center in substrate binding and activation (vide infra).

The reaction conditions were optimized using complexes **6** and **9** as catalysts. Increasing the pressure of the reactant gases to a total pressure of 4 bar (2 bar of each reactant gas) and the reaction time to 48 h resulted in an increase of the TONs to 475 and 587, respectively (Table 1, entries 11–13). These results set a new benchmark for the hydrogenation of N_2O to N_2 and H_2O (previously a TON of 417 at 3.5 bar H_2/3.5 bar N_2O at 70 °C were achieved with the Ru complex shown in Figure 1).[17]

Catalytic reduction of NO_x

The high stability and efficiency of the Rh–Pt complexes prompted us to investigate the hydrogenation of nitrogen oxide NO (Table 2, Figure 3). The chloride complex **3**, as well as the three best-performing complexes **6**, **7**, and **9** in the hydrogenation of N_2O were investigated as catalysts using tetrahydrofuran as solvent. The progress of the reaction was

Table 2: Catalytic reduction of NO by selected **[RhPt]** complexes.[a]

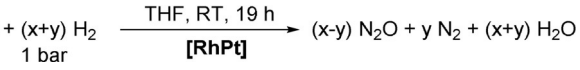

Entry	[RhPt]	TON′[b]
1	**3**	16
2	**6**	11
3	**7**	36
4	**9**	9[c]

[a] Conditions: [cat.] (3.0 mM), tetrahydrofuran (2 mL), total volume (50 mL). [b] Water formed during the reaction determined by Karl-Fischer titration. [c] With respect to one RhPt core.

monitored by quantification of the amount of water, which forms during the reaction. The combined $TON' = (TON_{(NO/N_2O)} + TON_{(N_2O/N_2)})$ for this transformation is given in Table 2. Surprisingly, the aquo complex **6** and ClTlCl-bridged dimer **9**, the most active N_2O reduction catalysts so far, performed poorly in the conversion of NO/H_2 to N_2O/H_2O (TON′ of ≈10, Table 2, entries 2 and 4). The neutral complexes **3** and **7** exhibit a higher activity with **3** affording a TON′ of 16 and **7** reaching a TON′ of 36 after 19 h (Table 2, entry 3). In all cases, N_2O was detected as one of the reaction products by GC-TCD.

Under optimized conditions, NO can be fully reduced to N_2 over the course of a week by the Rh–Pt triflate complex **7** (Figure 3a) as indicated by GC-TCD. The addition of PPh_3 poisons the catalyst showing that it proceeds in homogeneous phase. The generation of N_2O as an intermediate (GC-TCD, Figure S73) indicates a stepwise reduction, where NO is first converted to N_2O, followed by reduction to N_2 (GC-TCD, Figure S72).

To verify that this reaction can also be carried out under solvent-free conditions, complex **7** was deposited on activated carbon (**7@C** Figure 3a; Figures S74 and S75). The immobilized catalyst **7@C**, in presence of molecular sieves (pore size 4 Å) to trap water, was found to be as active as its homogenous counterpart (**7** in solution), and a combined TON′ = 34 was achieved (GC-TCD, Figure S76).

Remarkably, the more challenging substrate NO_2 can also be reduced by catalyst **7** (Figure 3b). The formation of NO and N_2O as reaction products were observed by GC-TDC, supporting again a stepwise reduction of NO_2 (Figure S77). For this transformation, a combined $TON'' = TON_{(NO_2/NO)} + TON'$ of 8 was observed. Therefore, we rank qualitatively the reaction rates for the individual conversions in the order $\nu_{(N_2O/N_2)} > \nu_{(NO/N_2O)} > \nu_{(NO_2/NO)}$. Very likely this reflects the stability of catalyst **7** against N_2O, NO, and NO_2. No decomposition of **7** was observed when a solution was stored under a mixture of N_2O and hydrogen by $^{31}P\{^1H\}$ NMR spectroscopy (vide supra). However, **7** decomposes within several days in an atmosphere of NO and hydrogen and within a day under NO_2 and hydrogen. The phosphine oxide of ligand **1** was the main decomposition product observed by $^{31}P\{^1H\}$ NMR spectroscopy.

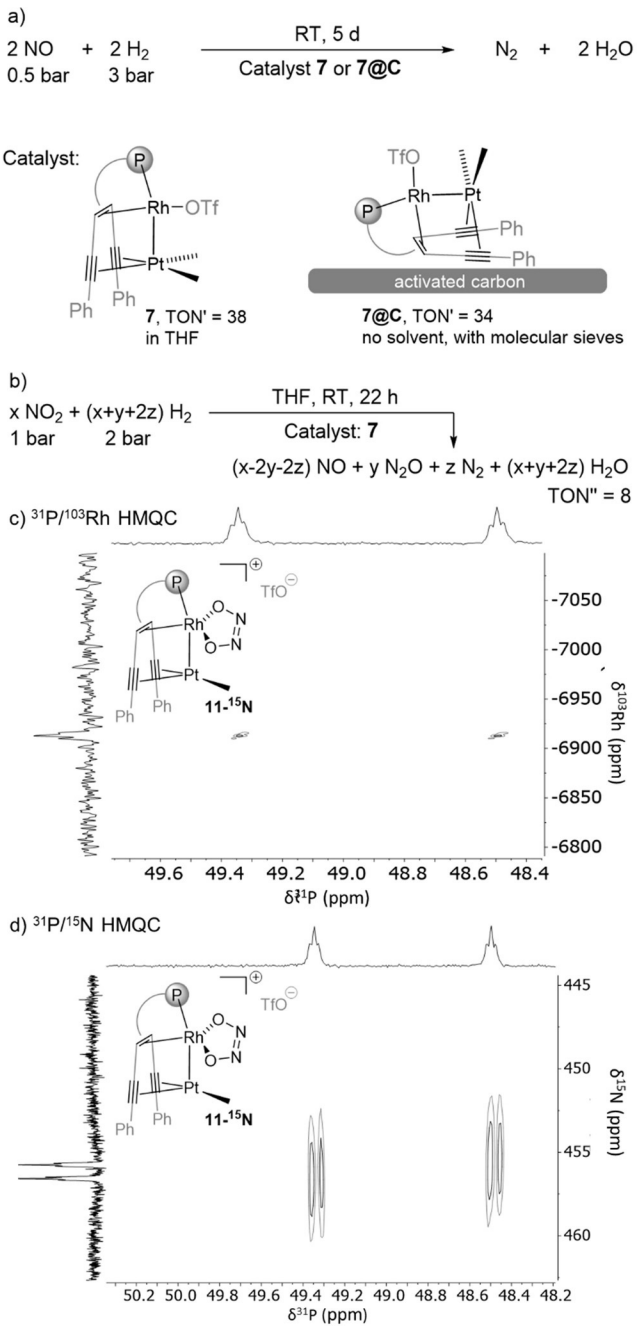

Figure 3. Optimized conditions for the catalytic reduction of a) NO and b) NO_2 with hydrogen and rhodium platinum triflate complex **7**. Reaction conditions for reduction of NO: **7** (6.5 mM), tetrahydrofuran (3 mL), total volume (50 mL). TON′ determined by GC-TCD and Karl-Fischer titration. Reaction conditions for reduction of NO_2: **7** (14 mM), [D_8]THF (0.5 mL), total volume (2.5 mL). TON″ was determined by ^1H NMR spectroscopy with mesitylene as an internal standard. NO and N_2O were detected by GC-TCD. The hyponitrite complex **11** was characterized as a key intermediate by c) $^{31}P/^{103}Rh$ HMQC and d) $^{31}P/^{15}N$ HMQC of ^{15}N-labeled **11**.

Mechanistic insight: stoichiometric experiments

The rhodium-platinum complexes **3**–**9** seemingly do not react with hydrogen (up to 5 bar) in tetrahydrofuran solution for weeks and neither rhodium nor platinum hydride species

were detected by ^{1}H NMR spectroscopy. However, scrambling experiments using a H_2/D_2 mixture, or H_2 and D_2O, with complex **7**, led to the detection of HD within minutes (Figures S78–S80). This demonstrates the capability of the rhodium-platinum triflate complex **7** to activate hydrogen and transfer hydrogen centers to a substrate molecule. Next, we investigated the interaction between **7** and NO by following the reaction using multinuclear NMR spectroscopy (Figures S81–S85) with the particular aim to better understand the nitrogen–nitrogen bond-forming step that must occur at some stage to generate N_2O from NO. A fast and quantitative formation of a new complex **11** is observed when **7** is placed under an atmosphere of NO in tetrahydrofuran. Complex **11** is remarkably stable in tetrahydrofuran solution and no decomposition was detectable by $^{31}P\{^{1}H\}$ NMR spectroscopy over several days. With ^{15}NO gas, the isotope-labeled complex **11-^{15}N** is formed, allowing a detailed spectroscopic analysis using $^{31}P/^{103}Rh$ and $^{31}P/^{15}N$ heteronuclear multiple quantum correlation (HMQC) experiments (Figure 3c,d). The ^{103}Rh NMR spectrum shows a resonance signal split into a triplet

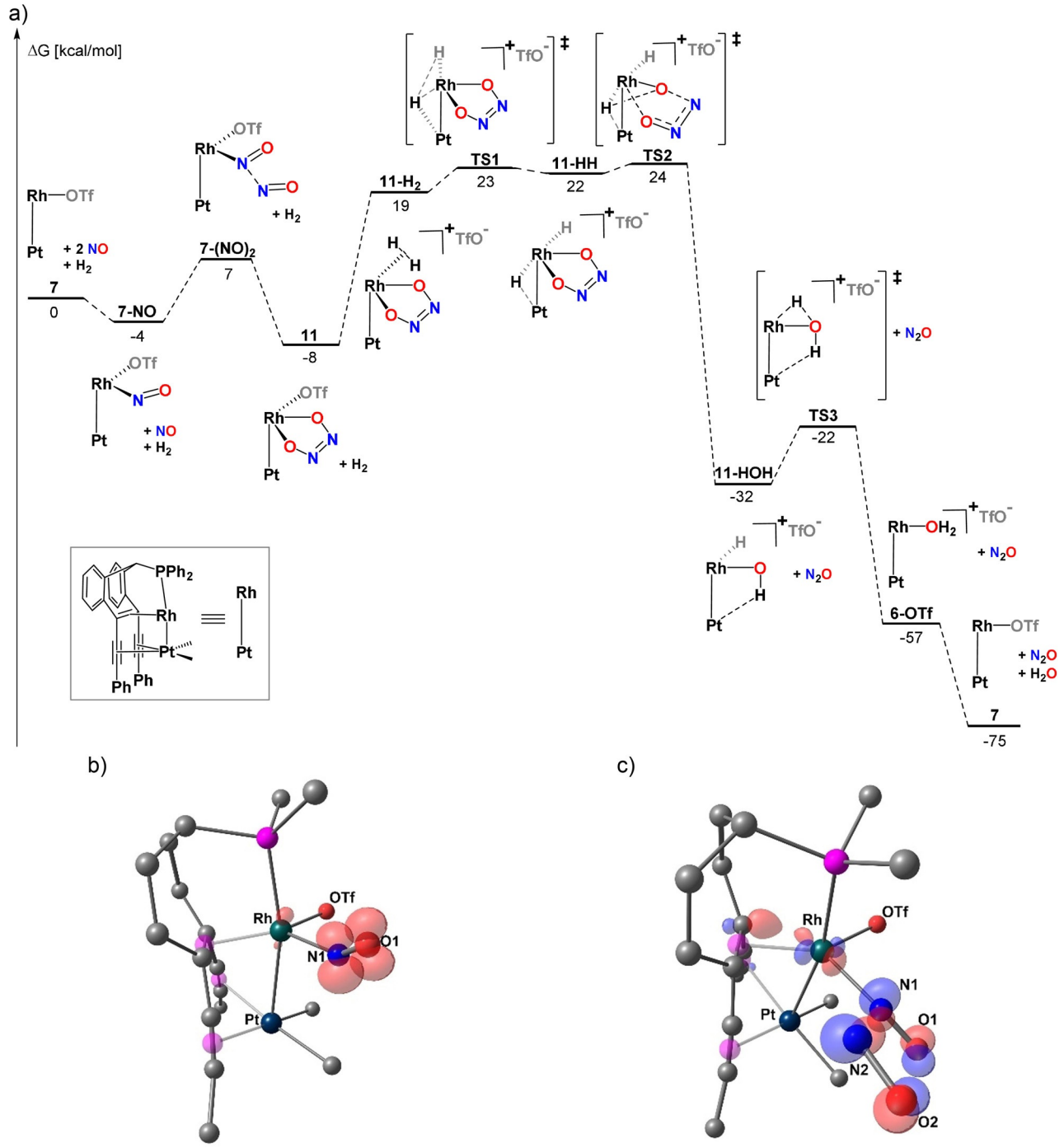

Figure 4. a) Minimum Energy Reaction Path (MERP) calculated with DFT for the conversion of 2 NO + H_2 to N_2O and H_2O using complex **7** as a catalyst. b) Plot of the calculated spin density in **7-NO**. c) Plot of the highest molecular orbital (HOMO) in **7-(NO)$_2$**.

which is caused by coupling between the ^{103}Rh nucleus and two equivalent ^{15}N nuclei ($^{2}J_{RhN} = 41.7$ Hz). Note that neither ^{195}Pt satellites could be observed nor a ^{195}Pt NMR spectrum could be measured. We attribute this to a larger ^{195}Pt chemical shift anisotropy (CSA) tensor in **11** compared to complexes **3**–**9**. It is a well-known phenomenon in ^{195}Pt NMR spectroscopy that larger CSA tensors may cause very fast relaxation resulting in resonance lines too broad to be detected.[28] ^{31}P{^{1}H} NMR spectroscopy of **11-^{15}N** shows a doublet of a triplet ($^{1}J_{PRh} = 171.4$ Hz, $^{3}J_{PN} = 4.5$ Hz) indicating two chemically equivalent ^{15}N centers. The observed coupling constant of $^{3}J_{PN} = 4.5$ Hz was utilized for polarization transfer in a ^{31}P/^{15}N HMQC experiment to prove the coupling between the nuclei (Figure 3d). The ^{15}N NMR spectrum of **11-^{15}N** shows a doublet ($^{2}J_{NRh} = 41.6$ Hz) of virtual triplets centered at $\delta^{15}N = 452.6$ ppm because the $^{3}J_{NRh}$ and $^{3}J_{NP}$ are by chance of the same value ($^{3}J_{NRh} = {}^{3}J_{NP} = 4.6$ Hz). In combination these results strongly indicate that complex **11** contains a *cis*-hyponitrite dianion, $N_2O_2^{2-}$, as ligand as a result of a reductive coupling reaction between two ^{15}NO molecules at the Rh center which is formally oxidized from Rh^{I} to Rh^{III} in this process (for comparison an aqueous solution of sodium *trans*-hyponitrite shows a resonance at $\delta^{15}N = 498.8$ ppm[29]). Pressurizing an NMR tube containing the hyponitrite complex **11** with 3 bar of hydrogen led to the formation of a triflate Rh^{I}–Pt^{II} complex within 21 hours postulated as **6-OTf**, with a water molecule coordinated to the rhodium center (Figure S86). The formation of hyponitrite complexes by reductive coupling of two equivalents of NO and the decomposition of these to N_2O has been intensively investigated but to the best of our knowledge, none of these reactions are catalytic.[30] The decomposition of hyponitrites to N_2O, especially in aqueous acidic solution in dependence of the pH, is well-established.[29,31]

Mechanistic insight: DFT calculations

According to DFT calculations (SMD/PBE0-D3/def2-SVP) (Figure 4), the formation of the hyponitrite complex **11** from complex **7** and two equivalents NO occurs in a stepwise manner. In the first exergonic addition of NO to **7**, a bent nitroso complex **7-NO** is obtained (-4 kcal mol^{-1}) in which NO coordinates with its N-center to Rh. The NO unit in **7-NO** retains largely its radical character as a plot of the calculated spin density shows (Figure 4b). In the second endergonic step ($+11$ kcal mol^{-1}), the second NO molecule attacks the Rh-bound NO at the N-center to form complex **7-(NO)$_2$** with an unusual Rh-NO-NO unit reminiscent of the π*-π* dimer formed when NO radicals are cooled below -160 °C or concentrated in confined spaces.[32] This is nicely illustrated by the plot of the HOMO of complex **7-(NO)$_2$** which is strongly localized on the N_2O_2 unit and corresponds to the bonding interaction between the π*-orbitals of each NO unit (Figure 4c). Subsequently, **7-(NO)$_2$** rearranges to the hyponitrite complex **11**. The overall reaction **7** + 2 NO → **11** is exergonic by $\Delta G = -8$ kcal mol^{-1}. No transition states could be located along the path **7** → **7-NO** → **7-(NO)$_2$** → **11** indicating that this part of the minimum energy reaction path (MERP) may be an almost barrierless process. The presented MERP (Figure 4a) is in agreement with the experimental observations but at present still remains one possibility and as such corresponds to a simplified model.

The displacement of the coordinated triflate anion by H_2 in the next reaction step to give the hydrogen complex **11-H$_2$** is rather endergonic ($\Delta G = 27$ kcal mol^{-1}) while the oxidative cleavage of H_2 proceeds via a low barrier at **TS1** ($\Delta G^{\ddagger} = 4$ kcal mol^{-1}) to give **11-HH**. In this dihydride complex one hydride is bound terminally to Rh and the other in a bridging μ_2-fashion over the Rh–Pt bond. The following step involves the transfer of the μ_2-H center to one oxygen center of the coordinated hyponitrite ligand to give the activated complex **TS2** ($\Delta G^{\ddagger} = 2$ kcal mol^{-1}) which decomposes to give N_2O and a hydrido hydroxo complex **11-HOH** in which the OH ligand takes a bridging position between Rh and Pt in such a fashion that O is bound to Rh and the H center has a contact to Pt. It is in these two steps, **11-H$_2$** → **11-HH** and **11-HH** → **11-HOH**, that the Pt center intervenes as a cooperative reaction center. The reaction **11-HH** to **11-HOH** + N_2O is strongly exergonic ($\Delta G = -54$ kcal mol^{-1}). The second product molecule, H_2O, is formed via transfer of the remaining hydride ligand to the hydroxo group, both bound at the Rh center to give the aquo complex **6-OTf** which was experimentally isolated as SbF_6^- salt (Figure 2). Displacement of the coordinated water molecule in **6-OTf** by the counter anion **OTf**$^-$ is exergonic and regenerates **7** ($\Delta G = 18$ kcal mol^{-1}) whereby the catalytic cycle is closed. The overall calculated reaction energy for $2NO + H_2 \rightarrow N_2O + H_2O$ of $\Delta G = -75$ kcal mol^{-1} is in very good agreement with the one obtained from experimental data ($\Delta G° = -71.13$ kcal mol^{-1}).[9]

Conclusion

A new family of stable heterodinucelar complexes was prepared using a ligand platform that was specifically designed to host two low-valent metal centers in close proximity. The compounds **3**–**9** contain a directly bonded Rh^{I}–Pt^{II} unit where both metal centers have a d^8 valence electron configuration. Quantum mechanical calculations indicate that this bond is best described as a dative Pt→Rh bond.

Among these dinuclear complexes, those which may liberate a free coordination site at the Rh center are active as catalysts in the hydrogenation ("reduction") of the nitrogen oxides NO_2, NO and N_2O which are converted to water and dinitrogen. Following the reaction between the catalyst and NO by NMR spectroscopy allowed us to unambiguously identify a hyponitrite complex as a key intermediate for the N–N bond forming-step which is crucial for the conversion of NO_x to N_2. Taking the experimental results into account, DFT calculations were preformed and allow us to make a proposition for a possible mechanism leading from 2 NO and H_2 to N_2O and H_2O. Although certainly oversimplified (for example, because specific interactions between the intermediates and solvent molecules and/or water, which forms during the reaction, were neglected) a MERP profile can be proposed which is roughly in accord with the experimental observa-

tions: NO_x is rapidly converted to hyponitrite in a reductive coupling step mediated at one metal center followed by slower hydrogenation in which both metal centers cooperate. A detailed investigation of the interaction between the Rh–Pt complexes and H_2 or the hydrogenation of N_2O to N_2 and H_2O is beyond the scope of this work and requires additional experimental results. In a previous study we demonstrated that rhodium hydride species may convert N_2O via a [Rh]-H···O-N=N interaction directly into [Rh]-OH and N_2[16] and similar mechanisms may apply here. Overall the insight gained from this study may be used to prepare significantly more active catalysts which may be achieved by (i) designing a ligand which is more robust against NO_x and in particular avoids phosphorus-containing binding sites and (ii) the preparation of neutral complexes in order to avoid poisoning of the active centers by the counter ion. Remarkably, immobilization of the molecular catalyst on a support did not lower its activity. It may therefore be possible to (i) prepare an active catalyst using the principles of molecular design, (ii) optimize the catalyst components and reaction conditions in homogeneous solution using high-resolution spectroscopy, and (iii) immobilize the molecular catalyst on an inert support material to give a heterogeneous catalyst with well-defined active sites.

Acknowledgement

We thank Frank Krumeich for the STEM picture of **7@C** and Christoph Neff, Bodo Hattendorf and Detlef Günther for the ICP-MS analysis of **7@C**. P.J., A.A., J.J.G.C., G.L., E.F., F.M., S.G., M.T., T.L.G. and H.G. acknowledge funding from the Swiss National Science Foundation (SNF 162437, 181966 and 192106) and Eidgenössische Technische Hochschule Zürich (ETH). I.F. acknowledges the Spanish Ministerio de Ciencia e Innovación for financial support (RED2018-102387-T and PID2019-106184GB-I00). Deposition Number(s) 2050091, 2050092, 2050093, 2050094, 2050095, 2050096, 2050097, 2050098, 2050099 contain the supplementary crystallographic data for this paper. These data are provided free of charge by the joint Cambridge Crystallographic Data Centre and Fachinformationszentrum Karlsruhe Access Structures service www.ccdc.cam.ac.uk/structures.

Acknowledgements

Open access funding provided by Eidgenossische Technische Hochschule Zurich.

Conflict of Interest

The authors declare no conflict of interest.

Keywords: bimetallic catalyst · hyponitrite complexes · nitrogen oxides · platinum · rhodium

[1] G. Myhre, D. Shindell in *Climate Change 2013: The Physical Science Basis. Contribution of Working Group I to the Fifth Assessment Report of the Intergovernmental Panel on Climate Change* (Eds.: T. F. Stocker, D. Qin, G. K. Plattner, M. Tignor, S. K. Allen, J. Boschung, A. Nauels, Y. Xia, V. Bex, P. M. Midgley), Cambridge University Press, Cambridge, United Kingdom and New York, NY, USA, **2013**.
[2] G. Lammel, H. Graßl, *Environ. Sci. Pollut. Res.* **1995**, *2*, 40–45.
[3] A. R. Ravishankara, J. S. Daniel, R. W. Portmann, *Science* **2009**, *326*, 123–125.
[4] T. Boningari, P. G. Smirniotis, *Curr. Opin. Chem. Eng.* **2016**, *13*, 133–141.
[5] a) V. N. Parmon, G. I. Panov, A. Uriarte, A. S. Noskov, *Catal. Today* **2005**, *100*, 115–131; b) J. Hansen, M. Sato, *Proc. Natl. Acad. Sci. USA* **2004**, *101*, 16109–16114.
[6] T. Keijer, V. Bakker, J. C. Slootweg, *Nat. Chem.* **2019**, *11*, 190–195.
[7] J. Pérez-Ramírez, F. Kapteijn, K. Schöffel, J. A. Moulijn, *Appl. Catal. B* **2003**, *44*, 117–151.
[8] D. S. Reay, E. A. Davidson, K. A. Smith, P. Smith, J. M. Melillo, F. Dentener, P. J. Crutzen, *Nat. Clim. Change* **2012**, *2*, 410–416.
[9] M. W. Chase, *Journal of Physical and Chemical Reference Data, Monograph*, *Vol. 9*, 4th ed., American Chemical Society, American Institute of Physics, National Institute of Standards and Technology, Woodbury, **1998**.
[10] a) F. Kapteijn, J. Rodriguez-Mirasol, J. A. Moulijn, *Appl. Catal. B* **1996**, *9*, 25–64; b) C. S. Swamy, J. Christopher, *Catal. Rev.: Sci. Eng.* **1992**, *34*, 409–425; c) V. I. Sobolev, G. I. Panov, A. S. Kharitonov, V. N. Romannikov, A. M. Volodin, K. G. Ione, *J. Catal.* **1993**, *139*, 435–443; d) T. W. Dann, K. H. Schulz, M. Mann, M. Collings, *Appl. Catal. B* **1995**, *6*, 1–10; e) T. Yamashita, A. Vannice, *J. Catal.* **1996**, *161*, 254–262; f) N. Russo, D. Fino, G. Saracco, V. Specchia, *Catal. Today* **2007**, *119*, 228–232.
[11] J. Kašpar, P. Fornasiero, N. Hickey, *Catal. Today* **2003**, *77*, 419–449.
[12] F. Gao, X. Tang, H. Yi, S. Zhao, C. Li, J. Li, Y. Shi, X. Meng, *Catalysts* **2017**, *7*, 199.
[13] a) Y. Xin, Q. Li, Z. Zhang, *ChemCatChem* **2018**, *10*, 29–41; b) J. Wang, H. Zhao, G. Haller, Y. Li, *Appl. Catal. B* **2017**, *202*, 346–354; c) S. Zhang, B. Zhang, B. Liu, S. Sun, *RSC Adv.* **2017**, *7*, 26226–26242.
[14] M. Thema, F. Bauer, M. Sterner, *Renewable Sustainable Energy Rev.* **2019**, *112*, 775–787.
[15] a) S. Roy, M. S. Hegde, S. Sharma, N. P. Lalla, A. Marimuthu, G. Madras, *Appl. Catal. B* **2008**, *84*, 341–350; b) A. Gluhoi, M. A. P. Dekkers, *J. Catal.* **2003**, *219*, 197–205; c) J. Arenas-Alatorre, A. Gómez-Cortés, M. Avalos-Borja, G. Díaz, *J. Phys. Chem. B* **2005**, *109*, 2371–2376; d) S. A. Carabineiro, B. E. Nieuwenhuys, *Surf. Sci.* **2001**, *495*, 1–7; e) H. Cassel, E. Glückauf, *Z. Phys. Chem. Abt. B* **1932**, *19*, 47.
[16] T. L. Gianetti, S. P. Annen, G. Santiso-Quinones, M. Reiher, M. Driess, H. Grützmacher, *Angew. Chem. Int. Ed.* **2016**, *55*, 1854–1858; *Angew. Chem.* **2016**, *128*, 1886–1890.
[17] R. Zeng, M. Feller, Y. Ben-David, D. Milstein, *J. Am. Chem. Soc.* **2017**, *139*, 5720–5723.
[18] a) N. Xu, E. G. Abucayon, D. R. Powell, G. B. Richter-Addo, *Nitric Oxide* **2016**, *52*, 16–20; b) W.-Y. Wu, C.-N. Hsu, C.-H. Hsieh, T.-W. Chiou, M.-L. Tsai, M.-H. Chiang, W.-F. Liaw, *Inorg. Chem.* **2019**, *58*, 9586–9591.
[19] S. Ghosh, H. Deka, Y. B. Dangat, S. Saha, K. Gogoi, K. Vanka, B. Mondal, *Dalton Trans.* **2016**, *45*, 10200–10208.
[20] a) G. B. Wijeratne, M. Bhadra, M. A. Siegler, K. D. Karlin, *J. Am. Chem. Soc.* **2019**, *141*, 17962–17967; b) G. B. Wijeratne, S. Hematian, M. A. Siegler, K. D. Karlin, *J. Am. Chem. Soc.* **2017**, *139*, 13276–13279.

[21] Y. Arikawa, T. Asayama, Y. Moriguchi, S. Agari, M. Onishi, *J. Am. Chem. Soc.* **2007**, *129*, 14160 – 14161.
[22] a) L. B. Maia, J. J. G. Moura, *Chem. Rev.* **2014**, *114*, 5273 – 5357; b) K. Brown, M. Tegoni, M. Prudêncio, A. S. Pereira, S. Besson, J. J. Moura, I. Moura, C. Cambillau, *Nat. Struct. Biol.* **2000**, *7*, 191 – 195.
[23] P. Jurt, O. G. Salnikov, T. L. Gianetti, N. V. Chukanov, M. G. Baker, G. Le Corre, J. E. Borger, R. Verel, S. Gauthier, O. Fuhr, K. V. Kovtunov, A. Fedorov, D. Fenske, I. V. Koptyug, H. Grützmacher, *Chem. Sci.* **2019**, *10*, 7937 – 7945.
[24] J. F. Hinton, *Magn. Reson. Chem.* **1987**, *25*, 659 – 669.
[25] C. W. Haigh, R. B. Mallion, *Prog. Nucl. Magn. Reson. Spectrosc.* **1979**, *13*, 303 – 344.
[26] C. Holloway, M. Melnik, *Open Chem.* **2011**, *9*, 501.
[27] a) "Catalyst Inhibition and Deactivation in Homogeneous Hydrogenation": D. Heller, A. H. M. de Vries, J. G. de Vries in *Handbook of Homogeneous Hydrogenation* (Eds.: H. G. de Vries, C. Elsevier), Wiley-VCH, Weinheim, **2007**, chap. 44, pp. 1483 – 1516; b) P. S. Hallmann, D. Evans, J. A. Osborn, G. Wilkinson, *Chem. Commun.* **1967**, 305; c) R. Bonnaire, L. Horner, F. Schumacher, *J. Organomet. Chem.* **1978**, *161*, C41; d) M. A. Esteruelas, J. Herrero, M. Martin, L. A. Oro, V. M. Real, *J. Organomet. Chem.* **2000**, *599*, 178.
[28] B. M. Still, P. G. A. Kumar, J. R. Aldrich-Wright, W. S. Price, *Chem. Soc. Rev.* **2007**, *36*, 665 – 686.
[29] M. J. Akhtar, J. A. Balschi, F. T. Bonner, *Inorg. Chem.* **1982**, *21*, 2216 – 2218.
[30] Y. Arikawa, M. Onishi, *Coord. Chem. Rev.* **2012**, *256*, 468 – 478.
[31] M. N. Hughes, *Quart. Rev.* **1968**, *22*, 1 – 13.
[32] D. Srivastava, C. H. Turner, E. E. Santiso, K. E. Gubbins, *J. Phys. Chem. B* **2018**, *122*, 3604 – 3614.

Manuscript received: July 21, 2021
Revised manuscript received: September 6, 2021
Accepted manuscript online: September 12, 2021
Version of record online: October 20, 2021

